CONTROL OF LASER RADIATION PARAMETERS

PACS numbers: 42.55.Wd; 42.60.Fc; 42.65.Re
DOI: 10.1070/QE2009v039n10ABEH014138

Picosecond pulse generation in a passively mode-locked Bi-doped fibre laser

A.A. Krylov, P.G. Kryukov, E.M. Dianov, O.G. Okhotnikov

***Abstract*. CW passive mode locking is achieved in a bismuth-doped fibre laser using a semiconductor saturable absorber mirror optimised for operation in the range 1100 – 1200 nm. The pump source is a cw ytterbium fibre laser (1075 nm, maximum output power of 2.7 W), and the pulse parameters can be tuned by varying the intracavity group velocity dispersion using a diffraction grating pair. Stable laser pulses are obtained with a duration down to $\tau_p \approx 1.1$ ps.**

Keywords: *bismuth-doped fibre laser, mode locking, SESAM, GVD compensation.*

1. Introduction

The ever increasing attention paid to the study of bismuth-doped optical fibres is associated with efforts to extend the wavelength range of fibre lasers and amplifiers to the second transmission window of silica (~ 1.3 μm). To date, Bi-doped fibre lasers have been made to operate in continuous regime between 1140 and 1215 nm [1 – 4] when pumped by a cw ytterbium fibre laser and in the range 1.3 – 1.5 μm [5 – 7] when pumped by a cw bismuth fibre laser or a cw Raman laser.

The IR luminescence spectrum of bismuth centres in optical fibres may extend from 1.1 to 1.7 μm [5, 8]. This gives grounds to expect passively mode-locked Bi-doped fibre lasers to be capable of generating ultrashort pulses, down to the subpicosecond level, which would make them an alternative to the well-known Cr : forsterite ultrashort-pulse solid-state laser [9]. In the wavelength range 1150 – 1170 nm, the shortest pulse duration, ~ 0.9 ps, has been achieved to date with a bismuth-doped aluminosilicate fibre laser operating in the soliton regime [10].

Previous work has demonstrated passively mode-locked operation of a Bi-doped fibre laser with an intracavity group velocity dispersion (GVD) compensator in the form of a pair of reflection diffraction gratings [11]. Passive mode locking was initiated and maintained by a semiconductor saturable absorber mirror (SESAM). The laser generated ~ 5-ps pulses at ~ 1180 nm. This paper addresses the operation of a SESAM mode-locked Bi-doped fibre laser with the intracavity GVD controlled by a diffraction grating pair. By optimising the GVD, we have achieved stable generation of picosecond pulses.

2. Experimental

We used isotropic single-mode silica fibre with an aluminium/bismuth codoped core (3 % Al_2O_3, 97 % SiO_2, NA ≈ 0.13, cut-off wavelength $\lambda_c = 1100$ nm). The fibre was drawn out from a preform fabricated by the SPCVD process [11, 12]. At $\lambda = 1160$ nm, the fibre had a fundamental-mode (LP_{01}) field diameter of 7.5 ± 0.2 μm and a second-order dispersion $\beta_2 \approx +1.4 \times 10^{-2}$ ps^2 m^{-1}. The bismuth concentration in the fibre core was 3×10^{18} cm^{-3} as determined by X-ray microanalysis, the absorption coefficient of the fibre in the range 1060 – 1080 nm was ~ 1.2 dB m^{-1}, and the on/off saturated gain reached ~ 0.4 dB m^{-1} at 1160 nm [12].

The configuration of the pulsed Bi-doped fibre laser with an intracavity GVD compensator in the form of a diffraction grating pair is shown in Fig. 1. The laser configuration is similar to that described previously [11].

One of the mirrors of the Fabry – Perot laser cavity was a SESAM. The SESAM structure was grown by molecular beam epitaxy on a GaAs substrate and was optimised for operation in the range 1100 – 1200 nm [13, 14]. The absorber operated under near-resonance conditions, with a high saturable-loss contrast. It is in this case that self-starting

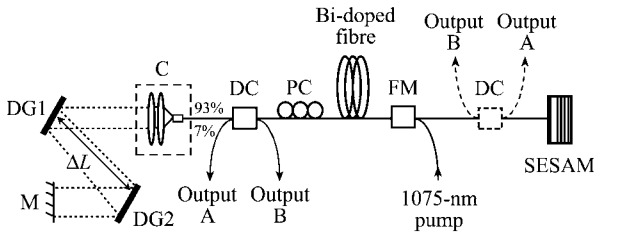

Figure 1. Pulsed Bi-doped fibre laser with an intracavity GVD compensator in the form of a diffraction grating pair: (FM) fibre multiplexer; (PC) single-mode Flexcore fibre polarisation controller; (DC) 7/93 (1160 nm) directional coupler for extracting radiation from the resonator; (DG1) and (DG2) reflection diffraction gratings; (M) multilayer dielectric mirror with ~ 100 % reflectance in the range 1140 – 1250 nm; (C) dual-lens collimator.

A.A. Krylov, P.G. Kryukov, E.M. Dianov Fiber Optics Research Center, Russian Academy of Sciences, ul. Vavilova 38, 119333 Moscow, Russia; e-mail: sokolak@mail.ru;
O.G. Okhotnikov Optoelectronics Research Center, Tampere University of Technology, Korkeakoulunkatu 3, Tampere, 33720 Finland; also with RafleKron Ltd., Ikmiestenkatu 17D 18, Tampere, 33710 Finland

Received 15 April 2009; revision received 25 June 2009
Kvantovaya Elektronika **39** (10) 882 – 886 (2009)
Translated by O.M. Tsarev

mode locking is possible in lasers with both anomalous and normal intracavity GVDs [13, 14].

The other mirror of the cavity had a multilayer dielectric coating with ~ 100 % reflectance in the range 1140 – 1250 nm. A gold-plated diffraction grating pair mounted between the mirror and fibre end was used to control the intracavity GVD. The polarisation state of the beam in the cavity was varied using a 0.5-m single-mode Flexcore fibre polarisation controller. All the passive components of the resonator were made of single-mode Flexcore fibre having a fundamental-mode (LP_{01}) field diameter of 7.3 ± 0.1 μm and a normal GVD $\beta_2 \approx +1.7 \times 10^{-2}$ ps^2 m^{-1} at 1160 nm. The splice losses between the active and passive fibres were within 0.2 dB.

The diffraction grating period was $d = 1$ μm (1000 lines per 1 mm). The beam was incident on the grating at 58°, and the first-order diffraction angle was $\theta' \approx 17.5°$ (the incident and diffracted beams were on the same side of the normal to the grating surface). The grating diffraction efficiency at 1160 nm was 92 % for the s-polarisation and 20 % for the p-polarisation. For the s-polarisation, the total loss in the GVD compensator, with allowance for the recoupling of light back into the fibre, was 1.7 dB, which is considerably less than the loss in the GVD compensator used previously [11]. This enabled a substantial reduction in the length of the Bi-doped fibre, down to 7 m.

The anomalous GVD due to the grating pair was evaluated as $\beta_2 \Delta L = -3(\text{ps}^2\ \text{m}^{-1})\Delta L$, where ΔL is the separation between the gratings along the beam direction [15]. The marked increase (by a factor of 3) in the magnitude of GVD compared to previous results [11] is due to the reduction in grating period and the increase in diffraction angle, θ' [15]. Therefore, the optimal grating separation, needed to compensate the normal GVD in the fibres, is ~ 10 cm, which is five times less than that obtained previously [11].

A portion of the laser output was extracted from the cavity by a directional coupler (DC) with a 7/93 power coupling ratio at 1160 nm and a 0.1-dB loss. Both of its output ports were used to measure laser parameters. The emission spectrum and average output power were measured at output A, and the intensity autocorrelation function was also analysed using output B. The position of the DC in the cavity was varied to optimise the quality of the laser pulses (in terms of duration and stability): the DC was located next to the GVD compensator (solid lines in Fig. 1) or at the SESAM (dashed lines).

The Bi-doped fibre laser was pumped by a purpose-designed cw ytterbium fibre laser with a maximum output power of 2.7 W at 1075 nm [11]. The pump beam was coupled into the Bi-doped fibre core through a fibre multiplexer, which effectively combined the 1075- and 1160-nm beams.

The temporal characteristics of laser pulses were measured using a Tektronix 7104 5-GHz analogue oscilloscope, a germanium photodetector with an intrinsic response time of 700 ps and an Inrad 5-14-LDA noncollinear phase matching intensity autocorrelator utilising a lithium niobate crystal (measurement range up to $\tau_{max} = 170$ ps). The autocorrelator output was fed to a LeCroy WaveSurfer 452 digital oscilloscope, which was used as a data logger. Spectral measurements were made with an Ando AQ6317B optical spectrum analyser, offering a resolution of down to 0.01 nm. The average beam power was measured by a Coherent FieldMaxII system equipped with a semiconductor sensor.

3. Results and discussion

We achieved cw passively mode-locked operation of the laser, with the pulse parameters significantly dependent on the magnitude and sign of the intracavity GVD and on the pump power. The generated ultrashort pulses were more stable when the DC was placed next to the SESAM, which was probably due to the more uniform loss distribution over the cavity in this configuration. The other parameters (the shapes of the autocorrelation trace and spectrum and the output power) remained essentially unchanged.

Figure 2a shows the intensity autocorrelation traces of laser pulses at different separations between the diffraction gratings for a Bi-doped fibre of length $L_{Bi} = 10$ m at a pump power $P_{pump} = 550$ mW. The corresponding emission spectra are displayed in Fig. 2b. Note that the passive fibre length in the cavity was 3.5 m, so the total GVD in the fibres of the laser was $D_2 = +0.2$ ps^2. To fully compensate the GVD, the separation between the diffraction gratings, ΔL, should be 6.7 cm.

It follows from Fig. 2a that reducing the grating separation and, accordingly, the magnitude of anomalous GVD, markedly lowers the autocorrelation pedestal [curves (*1*), (*2*)] and gives rise to a few side peaks. This is accompanied by broadening of the emission spectrum, but it remains bell-shaped and featureless [Fig. 2b, spectra (*1*), (*2*)]. Further reduction in grating separation, accompanied by a transition to normal intracavity GVD, leads to considerable pulse broadening and a marked distortion of the laser emission

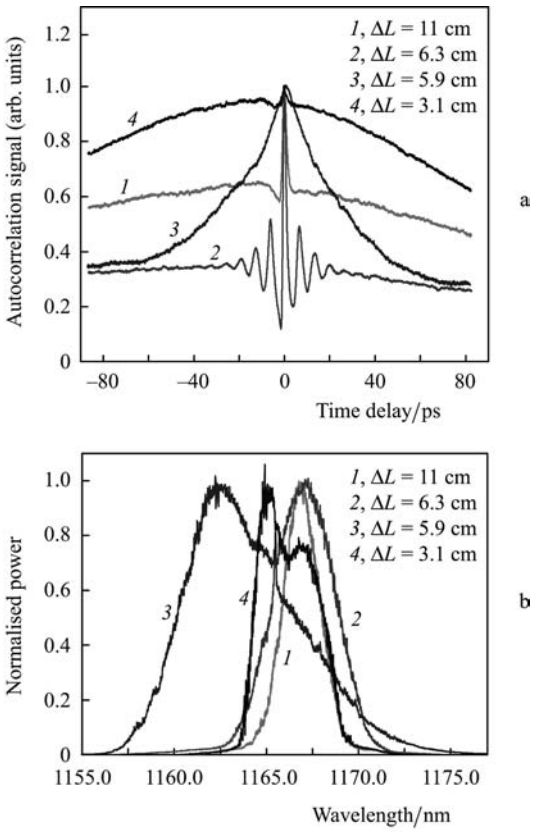

Figure 2. (a) Intensity autocorrelation traces and (b) emission spectra of the Bi-doped fibre laser at different separations between the diffraction gratings of the GVD compensator, ΔL. $L_{Bi} = 10$ m; $P_{pump} = 550$ mW; average output power $P_{out} = (1)$ 1.28, (*2*) 1.23, (*3*) 1.2 and (*4*) 1.3 mW.

spectrum [Figs 2a, b, curves (*3*), (*4*)]. Spectrum (*4*) is nearly rectangular in shape (which is better seen when the data is replotted on a logarithmic scale), characteristic of considerable normal intracavity GVD [16, 17]. The duration of laser pulses, which have a Gaussian envelope, is 171 ps. Curves (*3*) in Figs 2a and b seem to correspond to a nearly zero intracavity GVD. Therefore, the influence of self-phase modulation (SPM) and higher order dispersion on the pulse formation process contributes to considerable broadening of the spectrum and gives rise to a number of features and asymmetry [18]. Laser pulses are then unstable and have considerable (almost 100 %) amplitude modulation.

Lowering the pump power, P_{pump}, to 230 mW produces significant changes in the shape of the intensity autocorrelation function (Fig. 3a), whereas the shape of the emission spectrum remains almost unchanged (Fig. 3b). Indeed, the level of the pedestal and the area of its 'wings' decrease markedly, and the decrease depends on the intracavity GVD. These changes indicate that SPM has a significant effect on the pulse formation process. Like in a previous study [11], the pedestal seems to result from the fact that the contribution of SPM exceeds that of GVD, leading to a considerable nonlinear frequency modulation of the pulse, which is compensated only in its central part. As a consequence, pulse compression is incomplete, and a pedestal emerges. The development of several side peaks in the intensity autocorrelation function [Fig. 2a, curve (*2*)] with an increase in pulse power attests to complex phase modulation within the pulse, due to the influence of SPM.

Figure 4 shows oscilloscope traces of pulses at different intracavity GVD values and average output powers. In the case of a considerable normal intracavity GVD [Fig. 2, curve (*4*)], the pulse train has a period $T_{res} \approx 136$ ns and insignificant amplitude modulation at frequencies above 500 Hz (Fig. 4a), which points to high stability of the cw mode locking. Similar behaviour is observed in the case of anomalous intracavity GVD [Fig. 2, curves (*1*), (*2*)] at a pump power of 550 mW. Lowering the pump power to 230 mW [Fig. 3, curves (*1*)–(*3*)] slightly increases the pulse intensity modulation (Fig. 4b), but to a lesser extent. As mentioned above, nearly zero GVD [Fig. 2, curve (*3*); Fig. 3, curve (*4*)] is accompanied by an almost 100 % pulse intensity modulation. The higher pulse stability in comparison with previous results [11] is due to the substantial reduction in the lengths of the active and passive fibres and in passive intracavity losses. The latter factor seems to have a stronger effect on the amplitude stability of pulse trains.

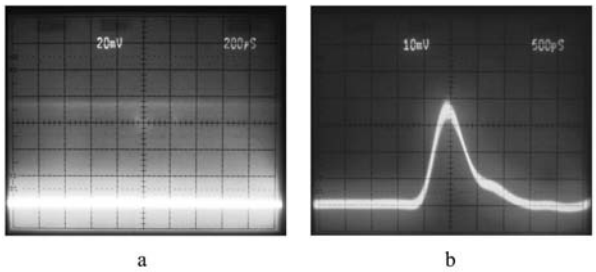

Figure 4. Oscilloscope traces of pulses generated by the Bi-doped fibre laser ($L_{Bi} = 10$ m): (a) $\Delta L = 3.1$ cm (normal GVD), $P_{out} = 1.3$ mW; (b) $\Delta L = 6.6$ cm (anomalous GVD), $P_{out} = 0.31$ mW.

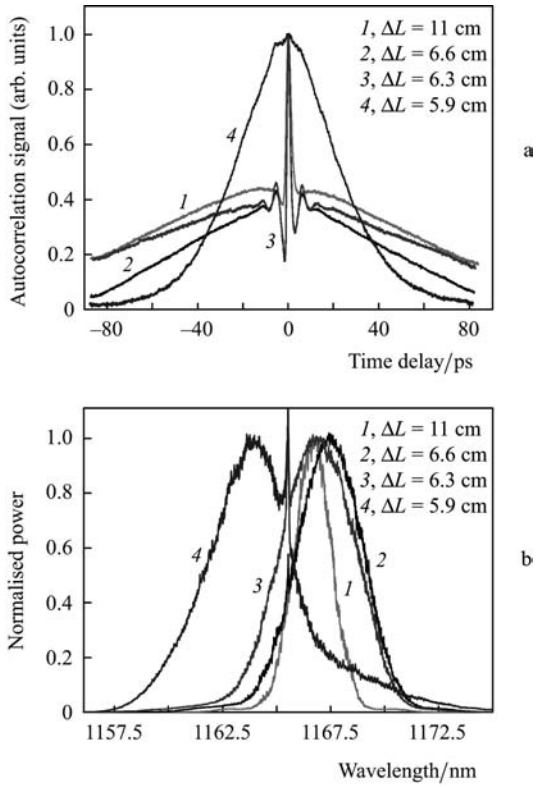

Figure 3. (a) Intensity autocorrelation traces and (b) emission spectra of the Bi-doped fibre laser at different separations between the diffraction gratings of the GVD compensator, ΔL. $L_{Bi} = 10$ m; $P_{pump} = 230$ mW; average output power $P_{out} =$ (*1*) 0.32, (*2*) 0.31, (*3*) 0.33 and (*4*) 0.3 mW.

Figure 5a presents the intensity autocorrelation traces with the lowest pedestal and smallest compressed pulse width at different lengths of the Bi-doped fibre. The corresponding emission spectra are displayed in Fig. 5b. As seen, reducing the length of the Bi-doped fibre considerably decreases the area of the uncompressed pedestal wings, with little effect on the average output power [Fig. 5a, curves (*1*), (*3*)]. This may be due to the reduction in the influence of SPM because of the decrease in nonlinear phase change and, as a consequence, in nonlinear pulse chirp with decreasing fibre length [18].

The narrow peaks near the centre of spectra (*3*) and (*4*) seem to be due to cw lasing in the cavity, but they are not Kelly sidebands, which emerge in spectra of soliton lasers [19, 20]. Note that, in all the cases represented in Fig. 5, further reducing the pump power leads to the degradation of mode locking.

To evaluate the minimum pulse duration, only the central, compressed portion of the autocorrelation is presented in Fig. 6. As seen, curves (*2*) and (*3*), corresponding to 10- and 8-m lengths of the Bi-doped fibre, coincide rather well, whereas curve (*1*), corresponding to a 15-m length of the fibre, is slightly broader. Curves (*2*) and (*3*) are well represented by a Gaussian fit [curve (*4*)] at negative time delays. The asymmetry of all the autocorrelations obtained is only due to the specific features of the autocorrelator used. In view of this, the pulse duration was evaluated from the best fit to the autocorrelation at negative time delays.

The minimum full width at half maximum (FWHM) of the intensity autocorrelation trace, τ_a, was determined to be 1.6 ps [Fig. 6, curves (*2*), (*3*)], which corresponds to a Gaussian pulse duration $\tau_p \approx 1.1$ ps (when an autocorrelation is fitted by a Gaussian, the FWHM Gaussian pulse

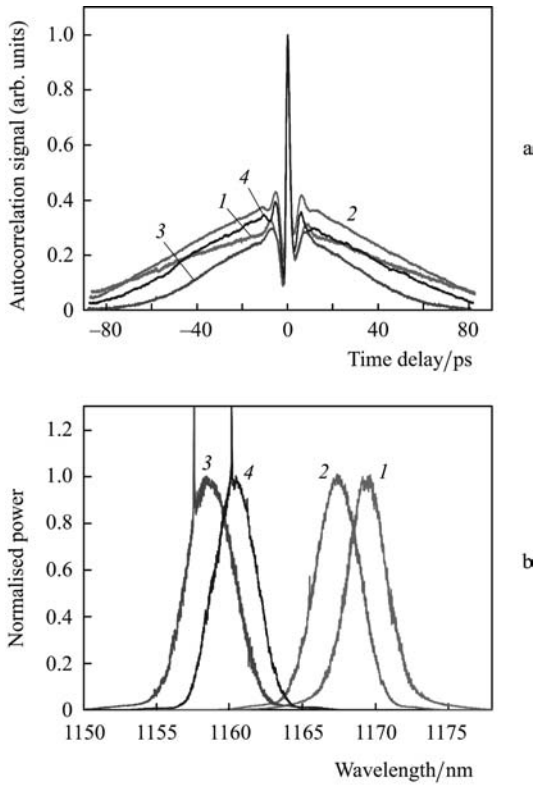

Figure 5. (a) Intensity autocorrelation traces and (b) emission spectra of the Bi-doped fibre laser at different Bi-doped fibre lengths (L_{Bi}) and pump powers (P_{pump}): (*1*) $\Delta L = 10.25$ cm, $P_{out} = 0.2$ mW, full width at half maximum of the spectrum $\Delta\lambda_{FWHM} \approx 2.9$ nm, $L_{Bi} = 15$ m, $P_{pump} = 190$ mW; (*2*) $\Delta L = 6.6$ cm, $P_{out} = 0.31$ mW, $\Delta\lambda_{FWHM} \approx 3.5$ nm, $L_{Bi} = 10$ m, $P_{pump} = 230$ mW; (*3*) $\Delta L = 6.3$ cm, $P_{out} = 0.24$ mW, $\Delta\lambda_{FWHM} \approx 3.8$ nm, $L_{Bi} = 8$ m, $P_{pump} = 370$ mW; (*4*) $\Delta L = 6.05$ cm, $P_{out} = 0.37$ mW, $\Delta\lambda_{FWHM} \approx 3.5$ nm, $L_{Bi} = 7$ m, $P_{pump} = 1140$ mW.

duration is a factor of $\sqrt{2}$ smaller than the autocorrelation duration [15]). The minimum pulse duration in the case of curve (*1*) was ≈ 1.4 ps. Note that, with increasing pump power, the autocorrelation duration and, accordingly, the pulse duration vary little, rising by less than 5 %.

The minimum time–bandwidth product, $C_p = \tau_p \Delta\nu_{FWHM}$, is 0.87 [Fig. 5, curve (*2*)], which is twice that for transform-limited Gaussian pulses (0.441) [15]. It is quite natural because the pedestal is due to specific spectral components, whose phases are rather intricate, nonlinear functions of frequency. It might therefore be expected that the pedestal can be eliminated by narrowing the emission spectrum, e. g. by placing a conventional slit near the cavity end mirror M. Our experiments show, however, that narrowing the spectrum raises intracavity losses and, hence, reduces the laser output power. In addition, this reduces the area of the uncompressed pedestal wings, which is equivalent to a decrease in pump power, but the wings persist to the point of mode locking disappearance.

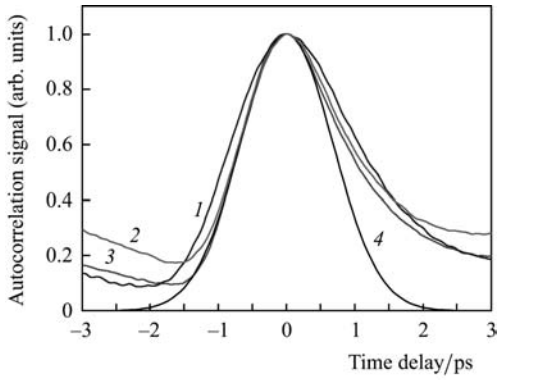

Figure 6. Autocorrelation of the compressed portion of pulses: (*1*) $\Delta L = 10.25$ cm, $P_{out} = 0.2$ mW, $\tau_p = 1.4$ ps, $L_{Bi} = 15$ m; (*2*) $\Delta L = 6.6$ cm, $P_{out} = 0.31$ mW, $\tau_p = 1.1$ ps, $L_{Bi} = 10$ m; (*3*) $\Delta L = 6.3$ cm, $P_{out} = 0.24$ mW, $\tau_p = 1.1$ ps, $L_{Bi} = 8$ m; (*4*) Gaussian fit.

Since curve (*3*) in Fig. 5 shows the entire autocorrelation pedestal, we can estimate the energy in the compressed (central) part of the pulse from the ratio of the area under its Gaussian fit to the entire autocorrelation area. This ratio is ~ 0.1, meaning that the energy in the compressed part of the pulse is one-tenth of the total output pulse energy, $E_{out} \approx 28$ pJ. Therefore, the energy and peak power of the compressed pulse in the cavity are $E_{in} \sim 40$ pJ and $P_{in} \sim 34$ W. This pulse power corresponds to a nonlinear length $L_{NL} = 7.6$ m (nonlinearity coefficient of the fibre $\gamma = 3.9 \times 10^{-3}$ W^{-1} m^{-1}) [11, 18], which leads to a round-trip nonlinear phase shift $\varphi_{NL} \approx 2L_{res}/L_{NL} \approx \pi$. At a pulse duration $\tau_p = 1.1$ ps, the dispersion length is $L_D = 32$ m [11, 18], that is, the nonlinear and dispersion lengths, characterising the contributions of SPM and GVD, respectively, are related by $N = \sqrt{L_D/L_{NL}} \approx 2.1$ [18]. This estimate demonstrates that both SPM and GVD play an important role in intracavity pulse compression.

It is also of interest to compare the measured output energy in the compressed peak with the maximum output soliton energy in a soliton laser with similar cavity parameters: $E_s = = 3.53|D_2|/(\gamma\tau_p L_{res})$ [20], where D_2 is the total intracavity GVD. Substitution of the experimental values $|D_2| \approx 3.76 \times 10^{-2}$ ps^2 and $L_{res} = 11.5$ m, corresponding to curve (*3*) in Fig. 5, yields $E_s = 2.6$ pJ, in reasonable agreement with the experimental estimate $E_p \approx 2.8$ pJ. It also follows from the above that, to raise the compressed pulse energy and eliminate the pedestal, one must reduce the fibre length in the cavity, maintaining the influence of SPM (the value of φ_{NL}) at the same level. The soliton period estimated as $Z_0 = (\pi/8\ln 2)\tau_p^2 L_{res}/|D_2|$ [20] is 216 m. Therefore, $8Z_0/L_{res} \gg 1$, which means that the first-order Kelly sidebands are offset from the centre of the spectrum by more than ten times its width [20].

It is also worth noting that varying the diameter of the beam spot on the SESAM had little effect on the laser operation. Optimal lasing conditions were achieved when the fibre end (polished) was butted against the SESAM surface. This indicates that the SESAM ensured mode-locked laser operation and had little or no effect on the temporal and spectral characteristics of generated pulses, which were governed by the mutual influence of GVD and Kerr-type nonlinear effects in the fibre.

4. Conclusions

Pulse compression in a bismuth-doped fibre laser was studied by controlling the intracavity GVD. CW passively mode-locked laser operation, initiated and maintained by a SESAM, was achieved using an intracavity GVD compensator in the form of a pair of reflection diffraction gratings.

The parameters of ultrashort pulses were shown to significantly depend on the magnitude and sign of the

intracavity GVD and the pump power. The laser parameters were optimised by adjusting the intracavity GVD to give stable ultrashort pulses with a duration down to $\tau_p \approx 1.1$ ps and a centre wavelength in the range 1158 – 1168 nm.

Further reduction in pulse duration and improvement in pulse quality via pedestal elimination are hindered by the significant influence of nonlinear effects in the long fibre cavity and the fairly high level of passive (nonsaturable) losses in the GVD compensator, which can only be reduced by using a rather long length of Bi-doped active fibre.

Acknowledgements. We thank K.M. Golant and A.V. Kholodkov for fabricating the Bi-doped fibre, I.A. Bufetov for providing the spectroscopic characteristics of the fibre, A.E. Levchenko for measuring the GVD of the fibres, B.L. Davydov for fabricating the fibre coupler and lens units used in this study, and A.V. Tausenev for help in acquiring the diffraction gratings for the GVD compensator.

References

1. Dianov E.M., Dvoyrin V.V., Mashinskii V.M., Umnikov A.A., Yashkov M.V., Gur'yanov A.N. *Kvantovaya Elektron.*, **35**, 1083 (2005) [*Quantum Electron.*, **35**, 1083 (2005)].
2. Razdobreev I., Bigot L., Pureur V., Favre A., Bouwmans G., Douay M. *Appl. Phys. Lett.*, **90**, 031103 (2007).
3. Rulkov A.B., Ferin A.A., Popov S.V., Taylor J.R., Razdobreev I., Bigot L., Bouwmans G. *Opt. Express*, **15**, 5473 (2007).
4. Dianov E.M., Shubin A.V., Melkumov M.A., Medvedkov O.I., Bufetov I.A. *J. Opt. Soc. Am. B*, **24**, 1749 (2007).
5. Dianov E.M., Firstov S.V., Khopin V.F., Guryanov A.N., Bufetov I.A. *Kvantovaya Elektron.*, **38** (7), 615 (2008) [*Quantum Electron.*, **38** (7), 615 (2008)].
6. Dvoyrin V.V., Medvedkov O.I., Mashinsky V.M., Umnikov A.A., Guryanov A.N., Dianov E.M. *Opt. Express*, **16**, 16971 (2008).
7. Bufetov I.A., Firstov S.V., Khopin V.F., Medvedkov O.I., Guryanov A.N., Dianov E.M. *Opt. Lett.*, **33**, 2227 (2008).
8. Dvoyrin V., Mashinsky V., Bulatov L., Bufetov I., Shubin A., Melkumov M., Kustov E., Dianov E., Umnikov A., Khopin V., Yashkov M., Guryanov A. *Opt. Lett.*, **31**, 2966 (2006).
9. Shcheslavskiy V., Yakovlev V.V., Ivanov A. *Opt. Lett.*, **26**, 1999 (2001).
10. Kivistö S., Puustinen J., Guina M., Okhotnikov O.G., Dianov E.M. *Electron. Lett.*, **44** (25), 1456 (2008).
11. Krylov I.A., Kryukov P.G., Dianov E.M., Okhotnikov O.G., Guina M. *Kvantovaya Elektron.*, **39** (1), 21 (2009) [*Quantum Electron.*, **39** (1), 21 (2009)].
12. Bufetov I.A., Golant K.M., Firstov S.V., Kholodkov A.V., Shubin A.V., Dianov E.M. *Appl. Opt.*, **47**, 4940 (2008).
13. Okhotnikov O., Pessa M. *J. Phys.: Condens. Matter*, **16**, S3108 (2004).
14. Okhotnikov O., Grudinin A., Pessa M. *New J. Phys.*, **6**, 177 (2004).
15. Diels J.-C., Rudolph W. *Ultrashort Laser Pulse Phenomena* (New York: Acad. Press, 1996).
16. Kutz J.N., Collings B.C., Bergman K., Tsuda S., Cundiff C., Knox W.H., Holmes P., Weinstein M. *J. Opt. Soc. Am. B*, **14**, 2681 (1997).
17. Herda R., Okhotnikov O. *IEEE J. Quantum Electron.*, **40**, 893 (2004).
18. Agrawal G.P. *Nonlinear Fiber Optics* (San Diego: Academic, 2001; Moscow: Mir, 1991).
19. Haus H.A., Ippen E.P., Tamura K. *IEEE J. Quantum Electron.*, **30**, 200 (1994).
20. Nelson L.E., Jones D.J., Tamura K., Haus H.A., Ippen E.P. *Appl. Phys. B*, **65**, 277 (1997).